Supporting Information

Ultrastable tetraphenyl-*p*-phenylenediamine–based covalent organic frameworks as platforms for high-performance electrochemical supercapacitors

Ahmed F. M. EL-Mahdy,[a,b] Mohamed Gamal Mohamed,[a,b] Tharwat Hassan Mansoure,[b,c,d] Hsiao-Hua Yu [c,d,] Tao Chen,[e] and Shiao-Wei Kuo [a,f]*

[a]Department of Materials and Optoelectronic Science, Center of Crystal Research, National Sun Yat-Sen University, Kaohsiung 80424, Taiwan.

[b]Chemistry Department, Faculty of Science, Assiut University, Assiut 71516, Egypt.

[c]Institute of Chemistry, Academia Sinica, 128 Academia Road Sec. 2, Nankang, Taipei 115, Taiwan.

[d]Department of Chemistry and Nanoscience and Technology Program, Taiwan International Graduate Program, Academia Sinica and National Taiwan University, Taipei 106, Taiwan.

[e]Ningbo Institute of Material Technology and Engineering, Chinese Academy of Science, Zhongguan West Road 1219, 315201 Ningbo, China

[f]Department of Medicinal and Applied Chemistry, Kaohsiung Medical University, Kaohsiung 807, Taiwan.

Email: kuosw@faculty.nsysu.edu.tw

S1. Materials

Chemicals and solvents were obtained from commercial sources and used as received. Pyrene (98%), tetrakis(triphenylphosphine)palladium(0) (99%), and palladium on activated carbon (10% Pd/C) were obtained from Acros. 1,1,2,2-Tetraphenylethylene (98%), bromine (99.99%), *n*-butanol (99.5%), *o*-dichlorobenzene (99%), acetic acid (99.8%), and 4-formylphenylboronic acid (95.0%) were purchased from Sigma–Aldrich. Hydrazine monohydrate (≥98%), and 1-fluoro- 4-nitrobenzene (99%) were obtained from Alfa Aesar. 1,4-Dioxane was purchased from J. T. Baker.

S2. Characterization

^{1}H and ^{13}C NMR spectra were recorded using an INOVA 500 instrument with DMSO-d_6 and $CDCl_3$ as solvents and tetramethylsilane (TMS) as the external standard. Chemical shifts are provided in parts per million (ppm). FTIR spectra were recorded using a Bruker Tensor 27 FTIR spectrophotometer and the conventional KBr plate method; 32 scans were collected at a resolution of 4 cm^{-1}. Solid state nuclear magnetic resonance (SSNMR) spectra were recorded using a Bruker Avance 400 NMR spectrometer and a Bruker magic-angle-spinning (MAS) probe, running 32,000 scans. Cross-polarization with MAS (CPMAS) was used to acquire ^{13}C NMR spectral data at 75.5 MHz. The CP contact time was 2 ms; ^{1}H decoupling was applied during data acquisition. The decoupling frequency corresponded to 32 kHz. The MAS sample spinning rate was 10 kHz. TGA was performed using a TA Q-50 analyzer under a flow of N_2. The samples were sealed in a Pt cell and heated from 40 to 800 °C at a heating rate of 20 °C min^{-1} under N_2 at a flow rate of 50 mL min^{-1}. PXRD was performed using a Siemens D5000 using monochromated $Cu/K\alpha$ ($\lambda = 0.1542$ nm). The sample was spread in a thin layer on the square recess of an XRD sample holder. The BET surface areas and porosimetry measurements of the prepared samples (ca. 20–100 mg) were performed using a Micromeritics ASAP 2020 Surface Area and Porosity analyzer. Nitrogen isotherms were generated through incremental exposure to ultrahigh-purity N_2 (up to ca. 1 atm) in a liquid N_2 (77 K) bath. FE-SEM was conducted using a JEOL JSM-7610F scanning electron microscope. Samples were subjected to Pt sputtering for 100 s prior to observation. TEM was

performed using a JEOL-2100 scanning electron microscope, operated at 200 kV. Molecular modeling was performed using Reflex, a software package for crystal determination from XRD patterns. Unit cell dimensions were first determined manually from the observed XRD peak positions using the coordinates.

S3. Synthetic Procedures

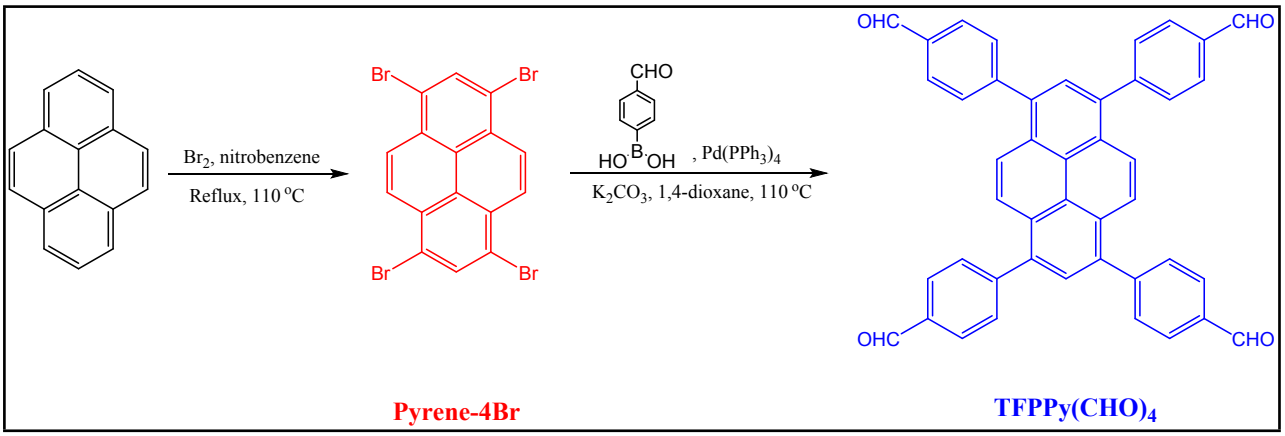

Scheme S1. Synthesis of 1,3,6,8-tetrakis(4-formylphenyl)pyrene [TFPPy(CHO)$_4$].

TFPPy(CHO)$_4$ was synthesized through Suzuki coupling, as described in literature.[S1] 1,3,6,8-Tetrabromopyrene (Pyrene-4Br) was prepared as described in the literature.[S2]

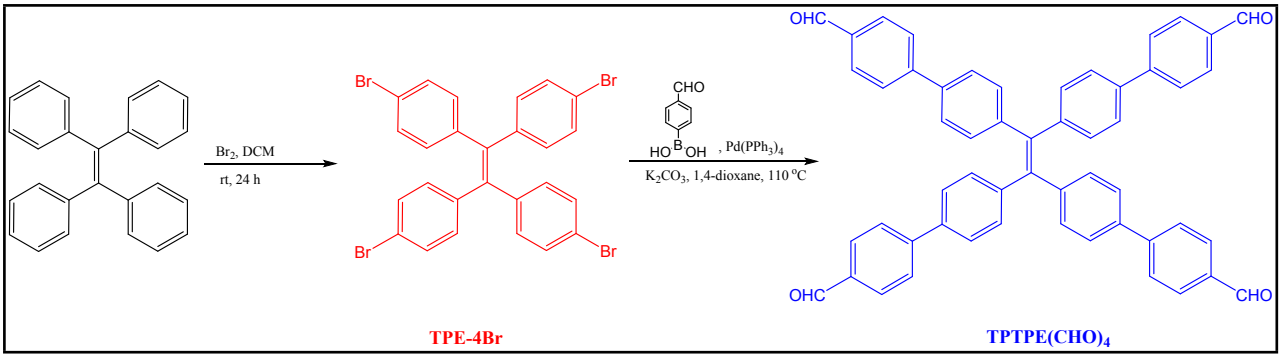

Scheme S2. Synthesis of 1,1,2,2-tetrakis[4-formyl-(1,1′-biphenyl)]ethane [TPTPE(CHO)$_4$].

Tetrakis(4-bromophenyl)ethylene (TPE-4Br)

TPE-4Br was synthesized according to a literature method,[S3] with slightly modification. Bromine (4.00 mL, 80.0 mmol) was added to a solution of tetraphenylethylene (3.32 g, 10.0 mmol) in glacial acetic acid (10 mL) and CH_2Cl_2 (20 mL) at 0 °C. The resulting mixture was stirred at room temperature for 3 h, and then poured into ice water (100 mL) and extracted with CH_2Cl_2. The organic phase was dried ($MgSO_4$) and the solvent evaporated under reduced pressure. The crude product was purified through recrystallization (MeOH) to give a white solid (18.0 g, 90 %); ^{1}H NMR ($CDCl_3$, 25 °C, 500 MHz): 6.85 (d, J = 8.56 Hz, 8H), 7.26 (d, J = 8.56 Hz, 8H) .^{13}C NMR ($CDCl_3$, 25 °C, 125 MHz): 121.50, 131.52, 132.98, 139.82, 141.69.

1,1,2,2-Tetrakis[4-formyl-(1,1´-biphenyl)]ethane [TPTPE(CHO)$_4$]

TPTPE(CHO)$_4$ was synthesized according to a published procedure.[S4] An aqueous solution of K_2CO_3 (1.66 g, 12 mmol) in water (15 mL) and tetrabutylammonium chloride (1 mL) were added to a solution of tetrakis(4-bromophenyl)ethylene (684 mg, 1.00 mmol) and 4-formylphenylboronic acid (900 mg, 6.00 mmol) in toluene (80 mL). $Pd(PPh_3)_4$ (10 mg) was added and then the mixture was stirred at 85 °C for 24 h. After cooling to room temperature, water was added and the organic layer was separated. Addition of MeOH to the organic layer precipitated a crude product. Recrystallization ($CHCl_3$/diethyl ether) gave a yellowish green solid (535 mg, 71%); ^{1}H NMR (DMSO-d_6, 25 °, 500 MHz): δ (ppm) = 10.03 (s, 4H), 7.96 (d, J = 8.3 Hz, 8H), 7.90 (d, J = 8.3 Hz, 8H), 7.69 (d, J = 8.3 Hz, 8H), 7.24 (d, J = 8.3 Hz, 8H).

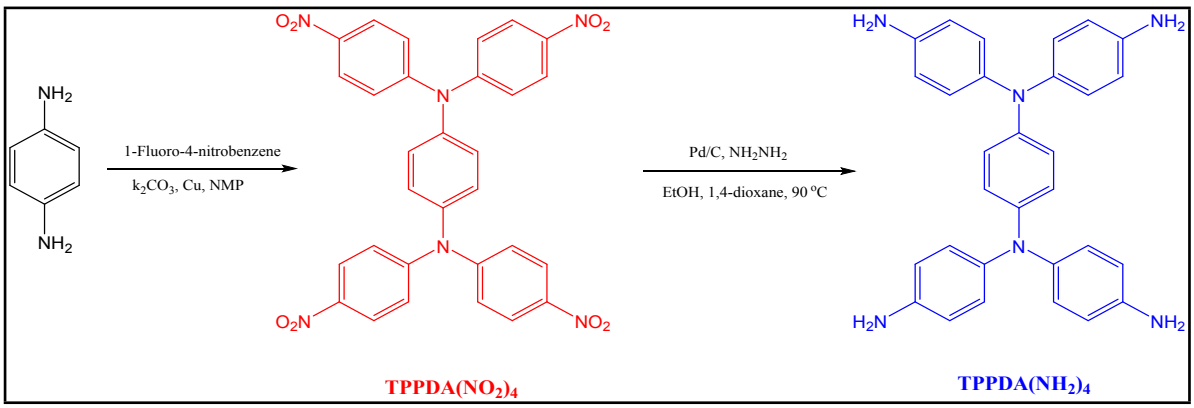

Scheme S3. Synthesis of N^1,N^1,N^4,N^4-tetrakis(4-aminophenyl)-*p*-phenylenediamine [TPPDA(NH_2)$_4$].

N^1,N^1,N^4,N^4-Tetrakis(4-nitrophenyl)-*p*-phenylenediamine [TPPDA(NO_2)$_4$]

p-Phenylenediamine (5.00 g, 46.0 mmol), 1-fluoro-4-nitrobenzene (39.1 g, 277 mmol), and K_2CO_3 (115 g, 832 mmol) were dissolved in 1-methyl-2-pyrrolidone (60 mL). The mixture was stirred while heating under reflux for 72 h and then cooled to ambient temperature to obtain crystals, which were washed sequentially with 1-methyl-2-pyrrolidone and water and then dried in air to obtain a solid (26.3 g, 96%). M.p.: 300 °C. Mass spectrum: *m*/*z* 592.

N^1,N^1,N^4,N^4-Tetrakis(4-aminophenyl)-*p*-phenylenediamine [TPPDA(NH_2)$_4$]

In a 100-mL two-neck round-bottom flask equipped with a stirring bar, TPPDA(NO_2)$_4$ (2.00 g, 3.37 mmol) and 10% Pd/C (0.20 g) were suspended in EtOH (20 mL) and 1,4-dioxane (40 mL) under a N_2 atmosphere. The suspension was heated at 90 °C for 15 min before hydrazine monohydrate (5.5 mL) was added slowly. The mixture was stirred at 90 °C for 36 h and then it was filtered to remove the Pd/C. The filtrate was cooled, giving greenish crystals, which were filtered off and dried under vacuum at 70 °C to obtain TPPDA(NH_2)$_4$ (0.8 g, 50%). FTIR (powder): 3456–3334, 3063–2836, 1626, 1500, 1256, 824 cm^{-1}. ^{1}H NMR (DMSO-d_6, 25 °C, 500 MHz): 4.81 (br s, 4NH_2, 8H), 6.46 (d, J = 8.50 Hz, 12H), 6.68 (d, J = 8.50 Hz, 8H). ^{13}C NMR (DMSO-d_6, 25 °C, 125 MHz): 145.17, 142.57, 138.05, 126.49, 120.96, 115.44.

TPPDA-TPPyr COF

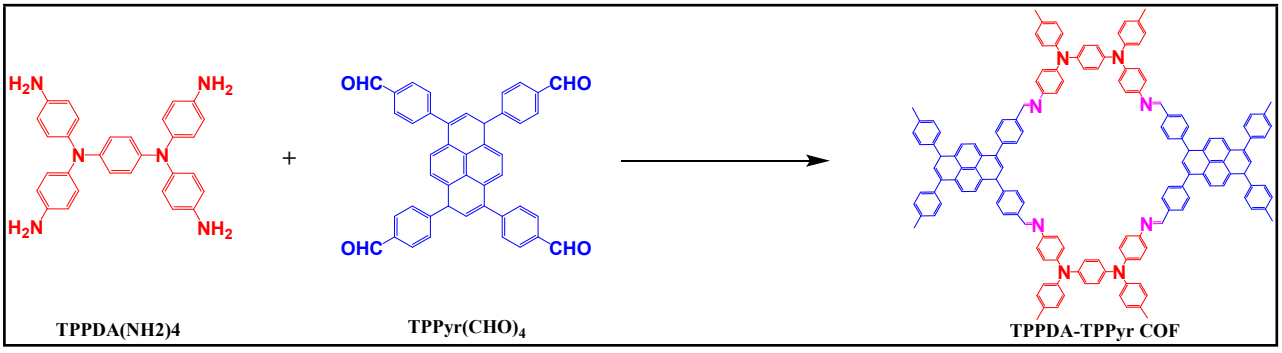

Scheme S4. Synthesis of the TPPDA-TPPyr COF.

In a 25-mL Schlenk storage tube, TPPDA(NH_2)$_4$ (100 mg, 0.210 mmol) and TPPyr(CHO)$_4$ (131 mg, 0.210 mmol) was dissolved in *n*-butanol (5 mL) and *o*-dichlorobenzene (5 mL) in the presence of acetic acid (6 M, 1 mL). The tube was sealed and degassed through three freeze/pump/thaw cycles. The tube was sealed off by flame and heated at 120 °C for 3 days. After cooling to room temperature, the tube was opened and the precipitate filtered and washed two times with *n*-butanol, THF, and acetone respectively. The solid was dried under vacuum at 120 °C overnight to afford TPPDA-TPPyr COF as an orange powder.

TPPDA-TPTPE COF

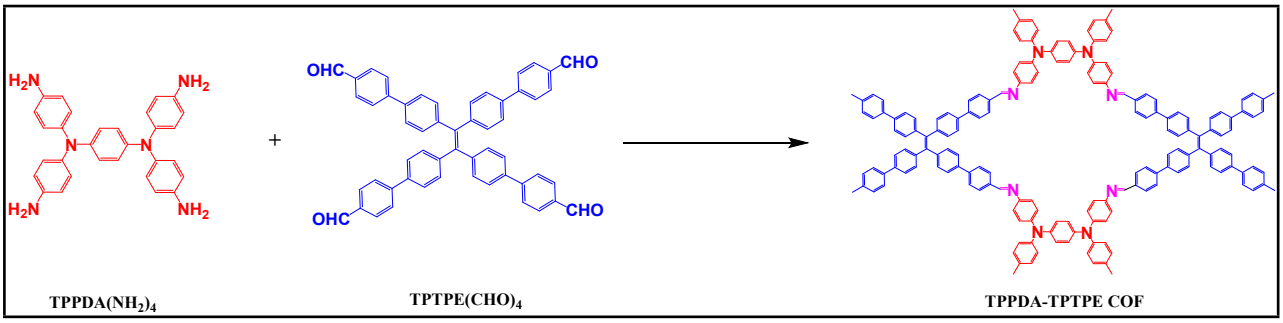

Scheme S5. Synthesis of the TPPDA-TPTPE COF.

In a 25-mL Schlenk storage tube, TPPDA(NH_2)$_4$ (100 mg, 0.210 mmol) and TPTPE(CHO)$_4$ (156 mg, 0.210 mmol) was dissolved in *n*-butanol (5 mL) and *o*-dichlorobenzene (5 mL) in the presence of acetic acid (6 M, 1 mL). The tube was sealed and degassed through three freeze/pump/thaw cycles. The tube was sealed off by flame and heated at 120 °C for 3 days. After cooling to room temperature, the tube was opened and the precipitate was filtered and washed two times with *n*-butanol, THF and acetone, respectively. The solid was dried under vacuum at 120 °C overnight to afford TPPDA-TPTPE COF as an orange powder.

S4. Spectral Profiles of TPPDA(NH_2)$_4$

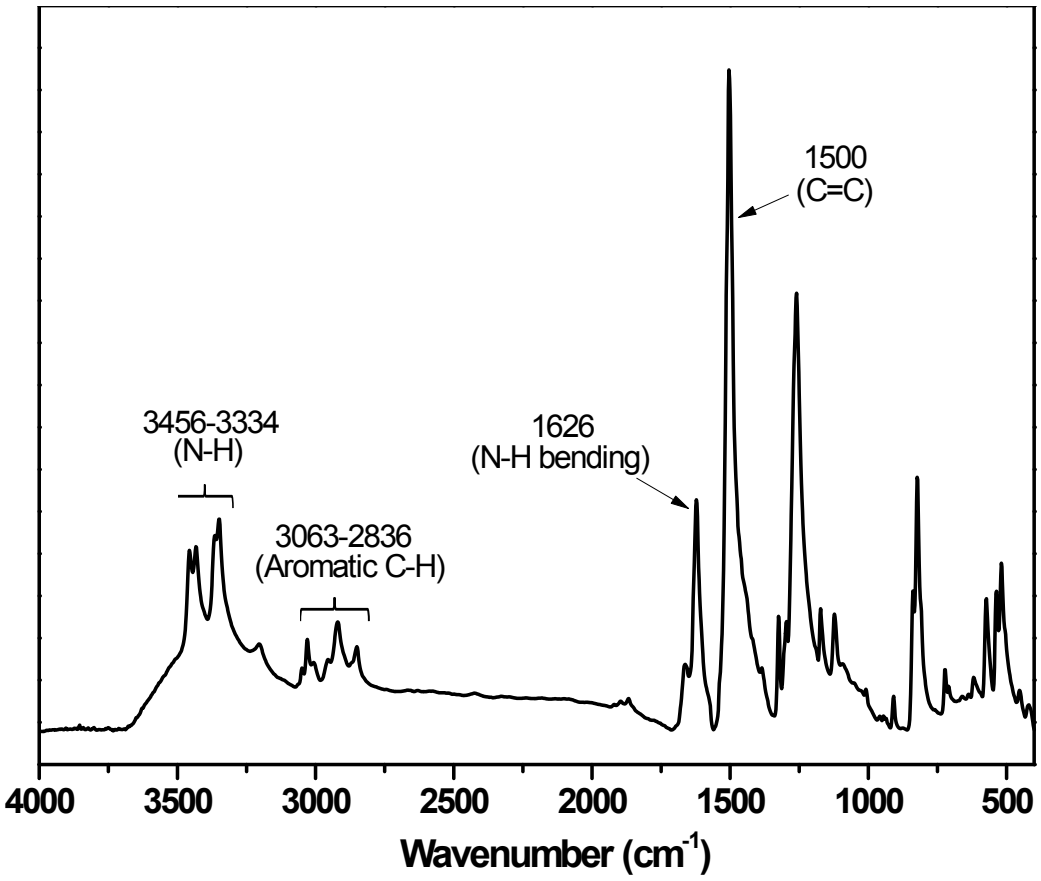

Fig. S1. FTIR spectrum of TPPDA$(NH_2)_4$.

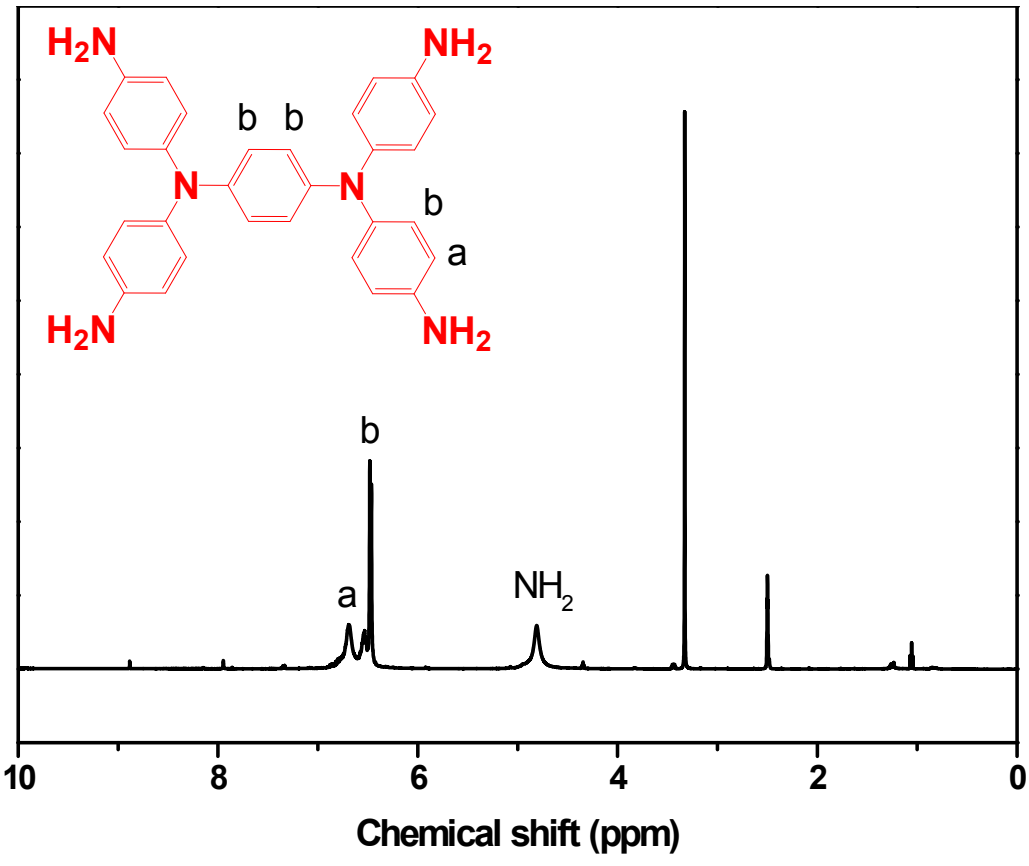

Fig. S2. ^{1}H NMR spectrum of TPPDA$(NH_2)_4$.

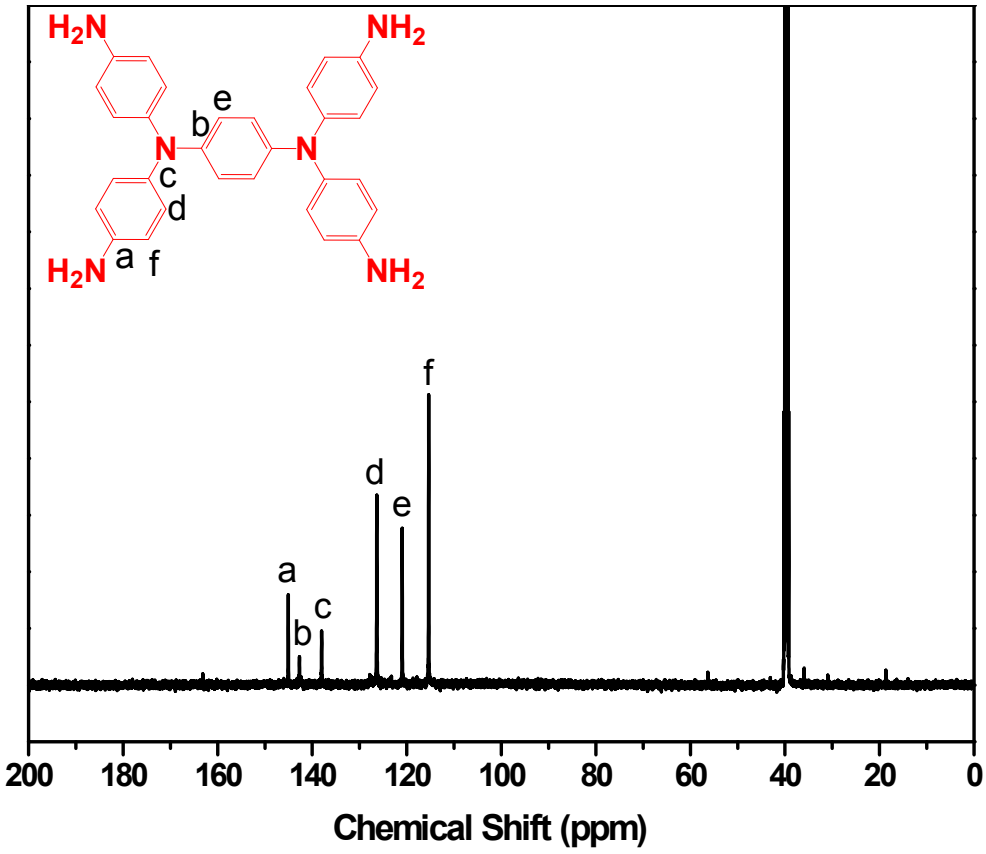

Fig. S3. ^{13}C NMR spectrum of TPPDA$(NH_2)_4$.

S5. FTIR Spectral Profiles of Monomers and COFs

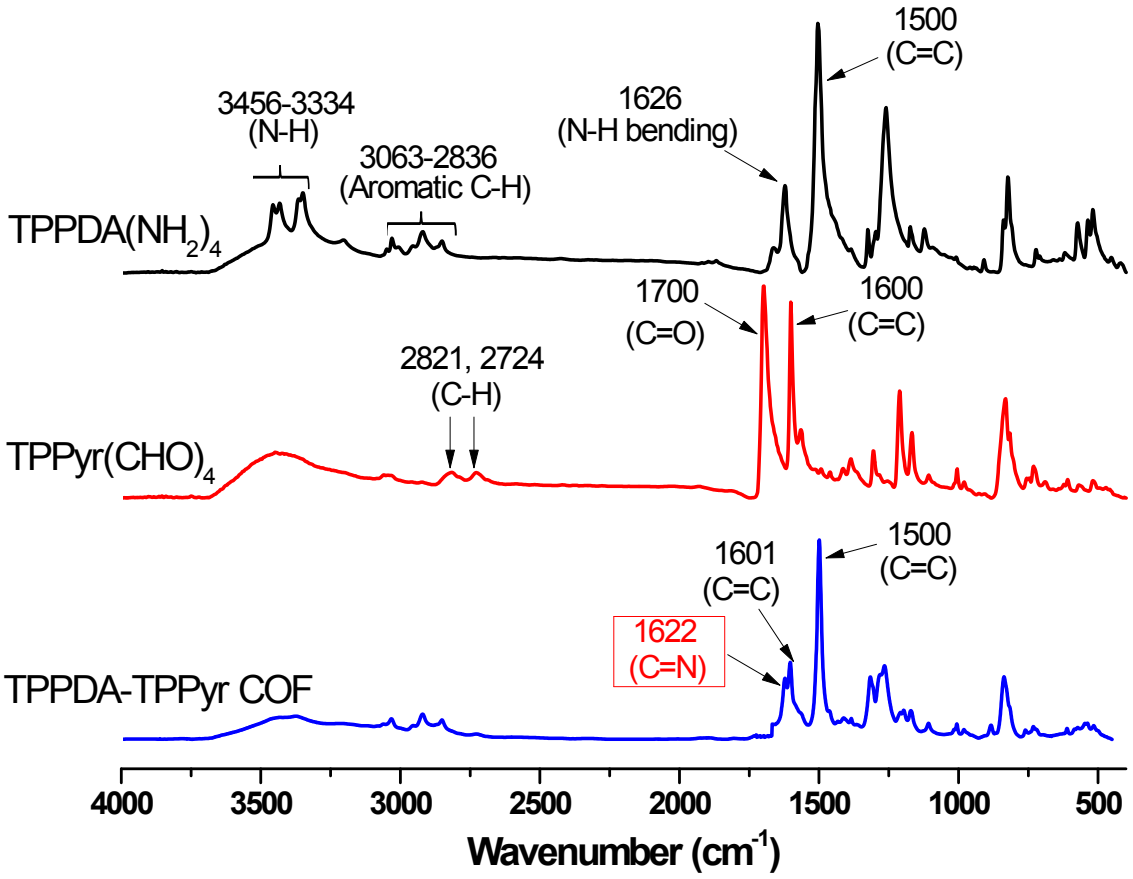

Fig. S4. FTIR spectra of $TPPDA(NH_2)_4$, $TPPyr(CHO)_4$, and the TPPDA-TPPyr COF.

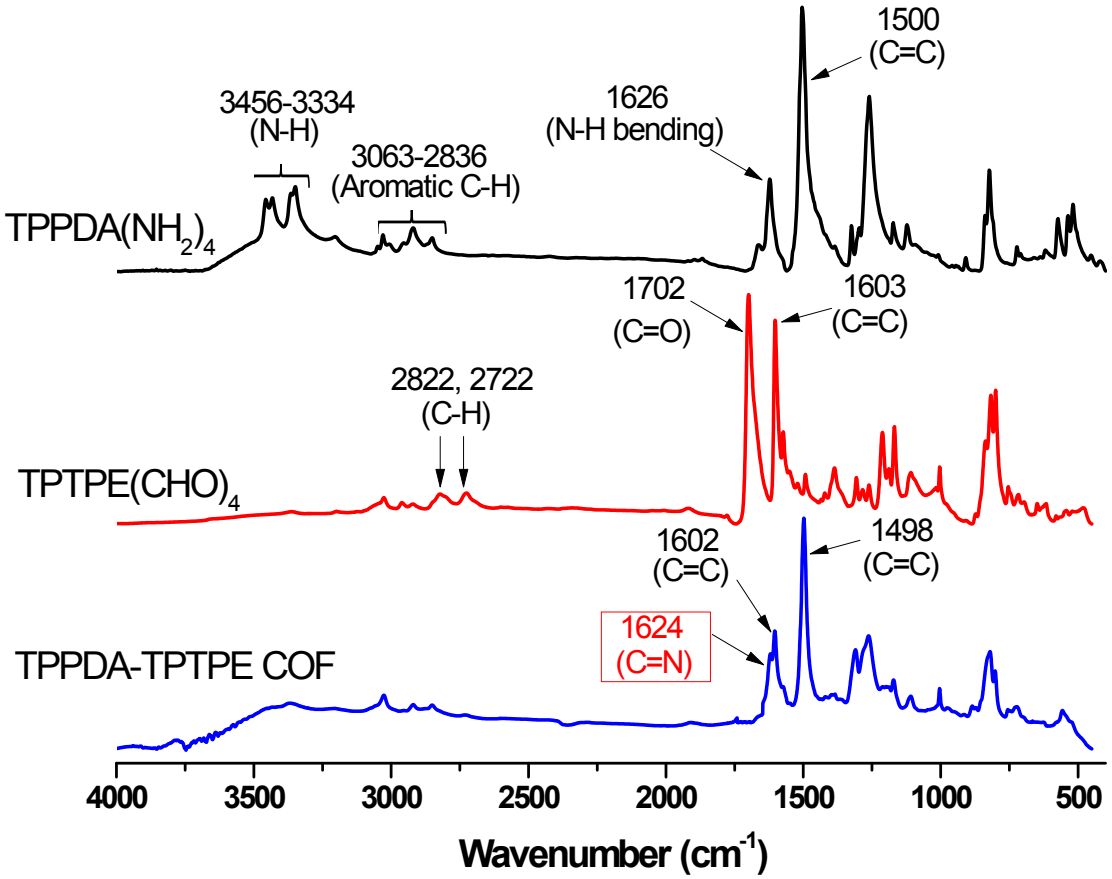

Fig. S5. FTIR spectra of $TPPDA(NH_2)_4$, $TPTPE(CHO)_4$, and the TPPDA-TPTPE COF.

S6. Solid-state ^{13}C CP MAS NMR Spectra

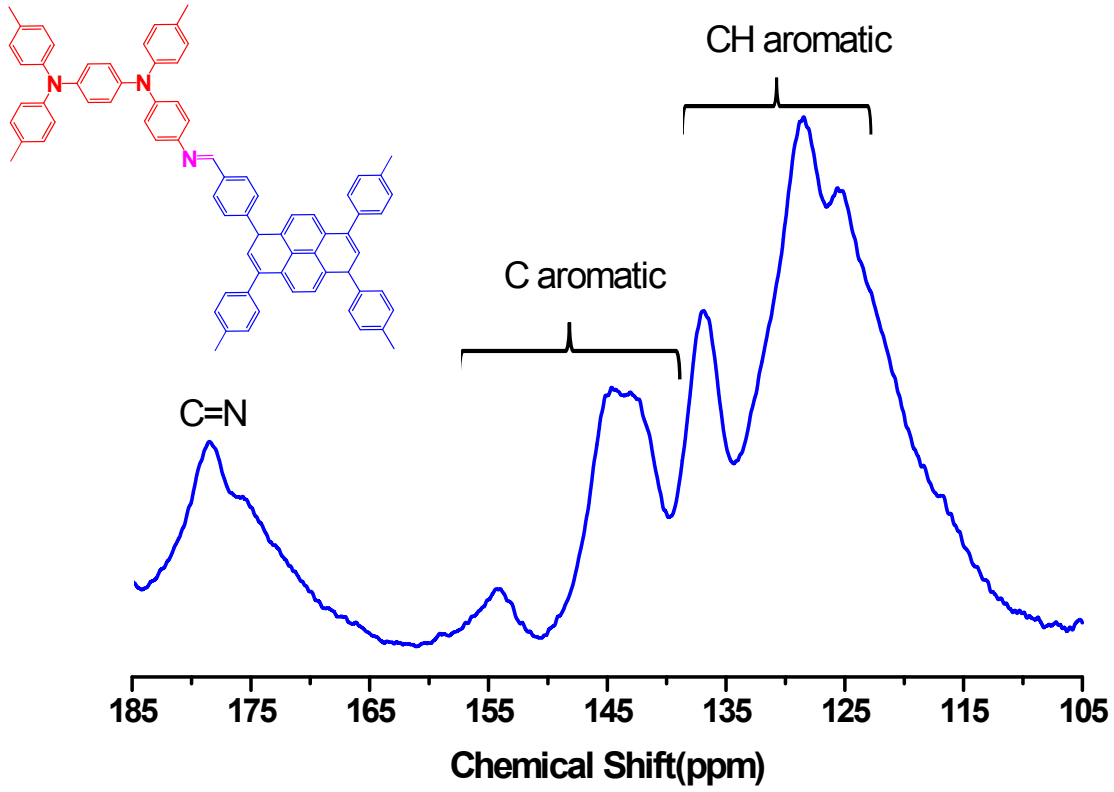

Fig. S6. ^{13}C Cross-polarization magic-angle-spinning solid state NMR spectrum of the TPPDA-TPPyr COF.

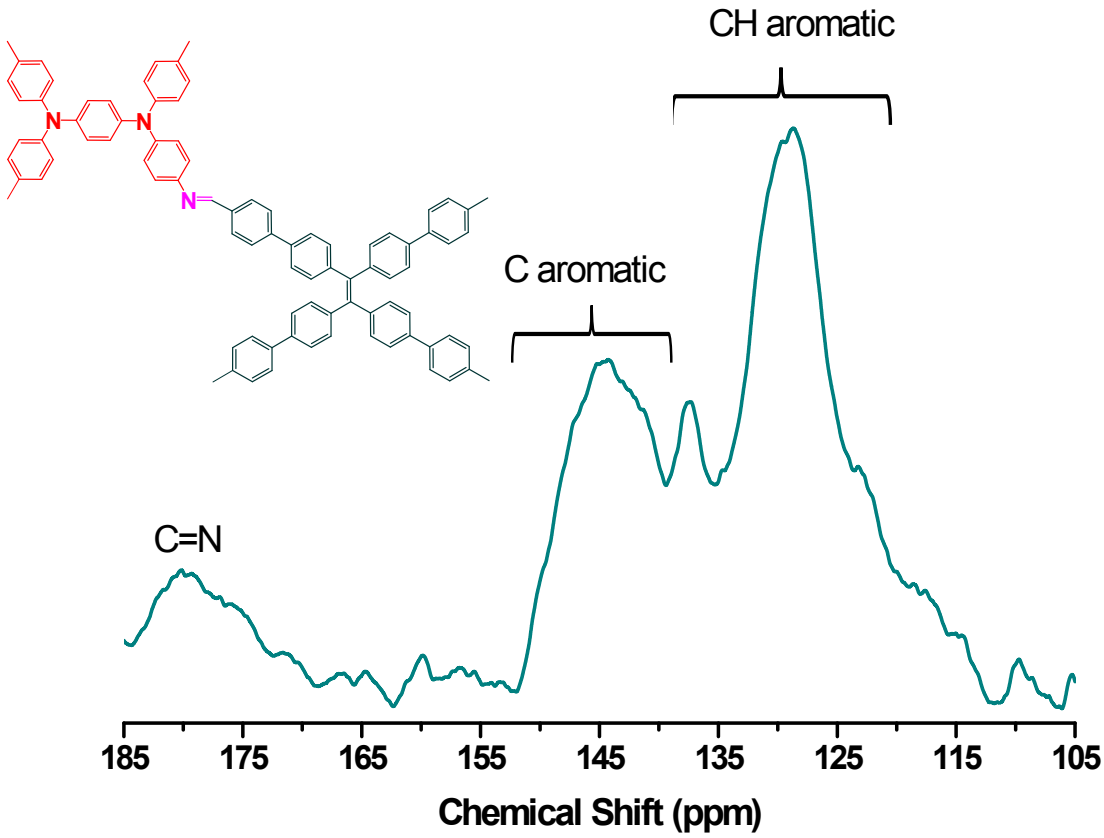

Fig. S7. ^{13}C Cross-polarization magic-angle-spinning solid state NMR spectrum of the TPPDA-TPTPE COF.

S7. Thermal Gravimetric Analysis

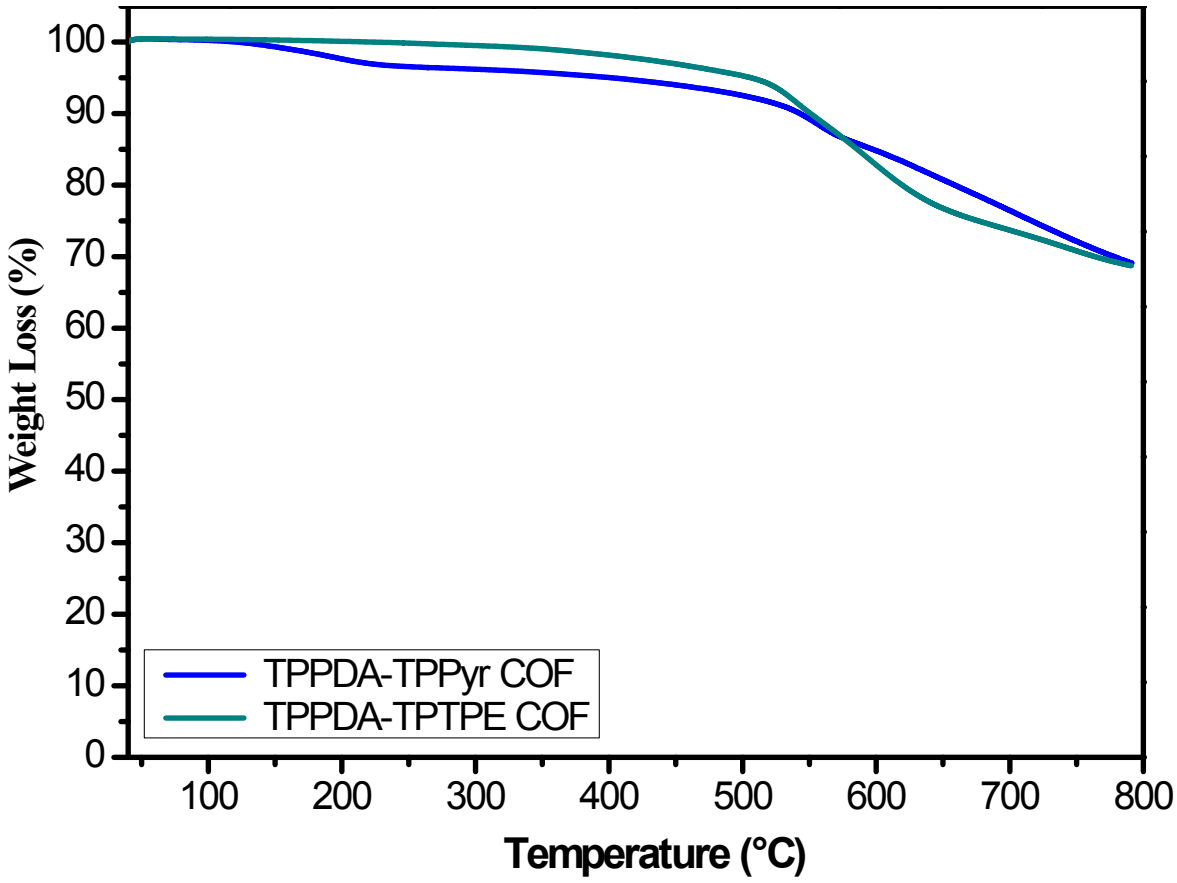

Fig. S8. TGA analyses of the TPPDA-TPPyr and TPPDA-TPTPE COFs.

Table S1. Values of $T_{d10\%}$ and Char yield of COFs.

	$T_{d10\%}$ (℃)	Char yield (%)
TPPDA-TPPyr COF	543	70
TPPDA-TPTPE COF	551	68

S8. Transmission Electron Microscopy (TEM)

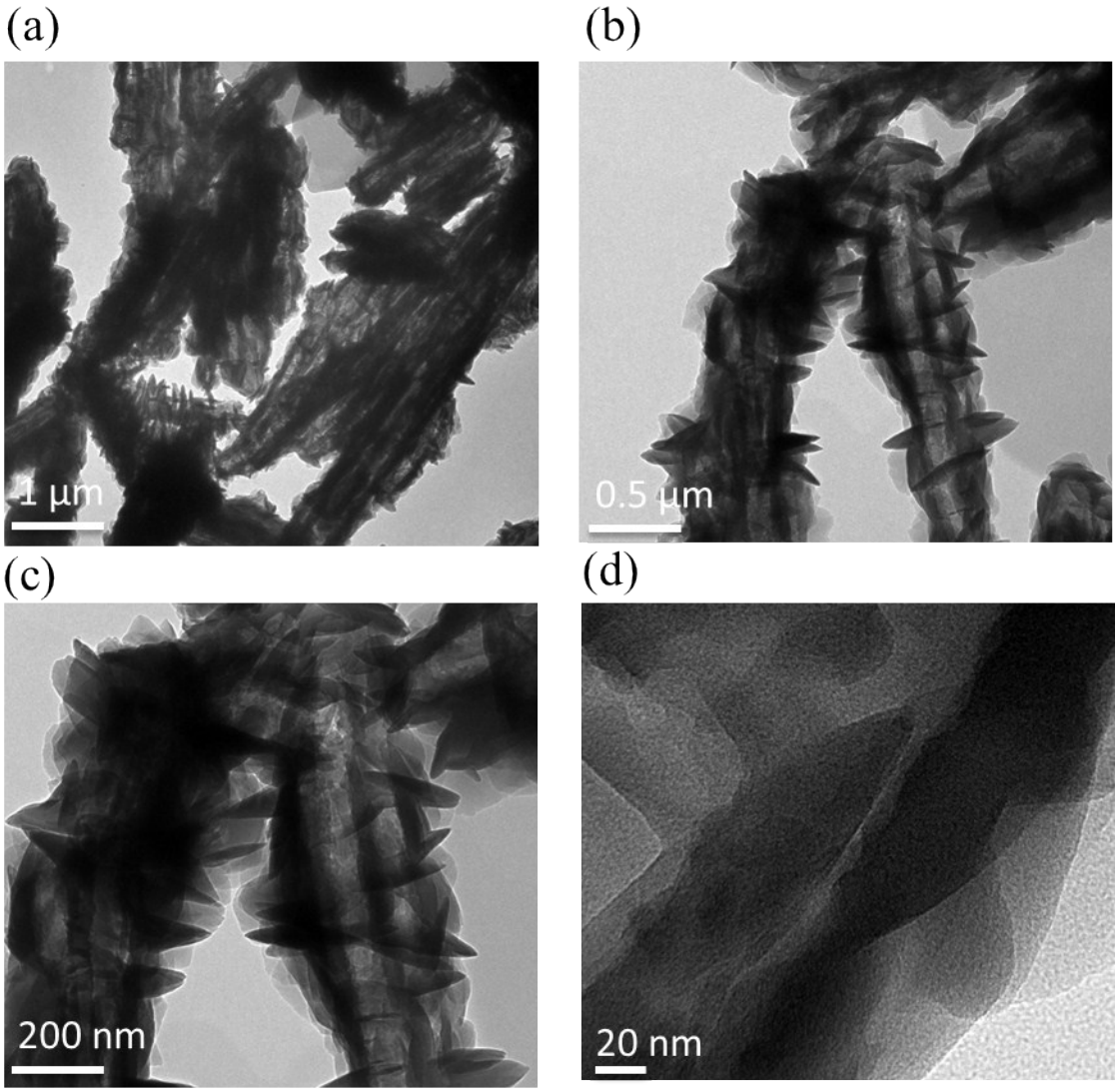

Fig. S9. TEM images of the TPPDA-TPPyr COF recorded at various magnifications: (a) 1 µm, (b) 0.5 µm, (c) 200 nm, and (d) 20 nm.

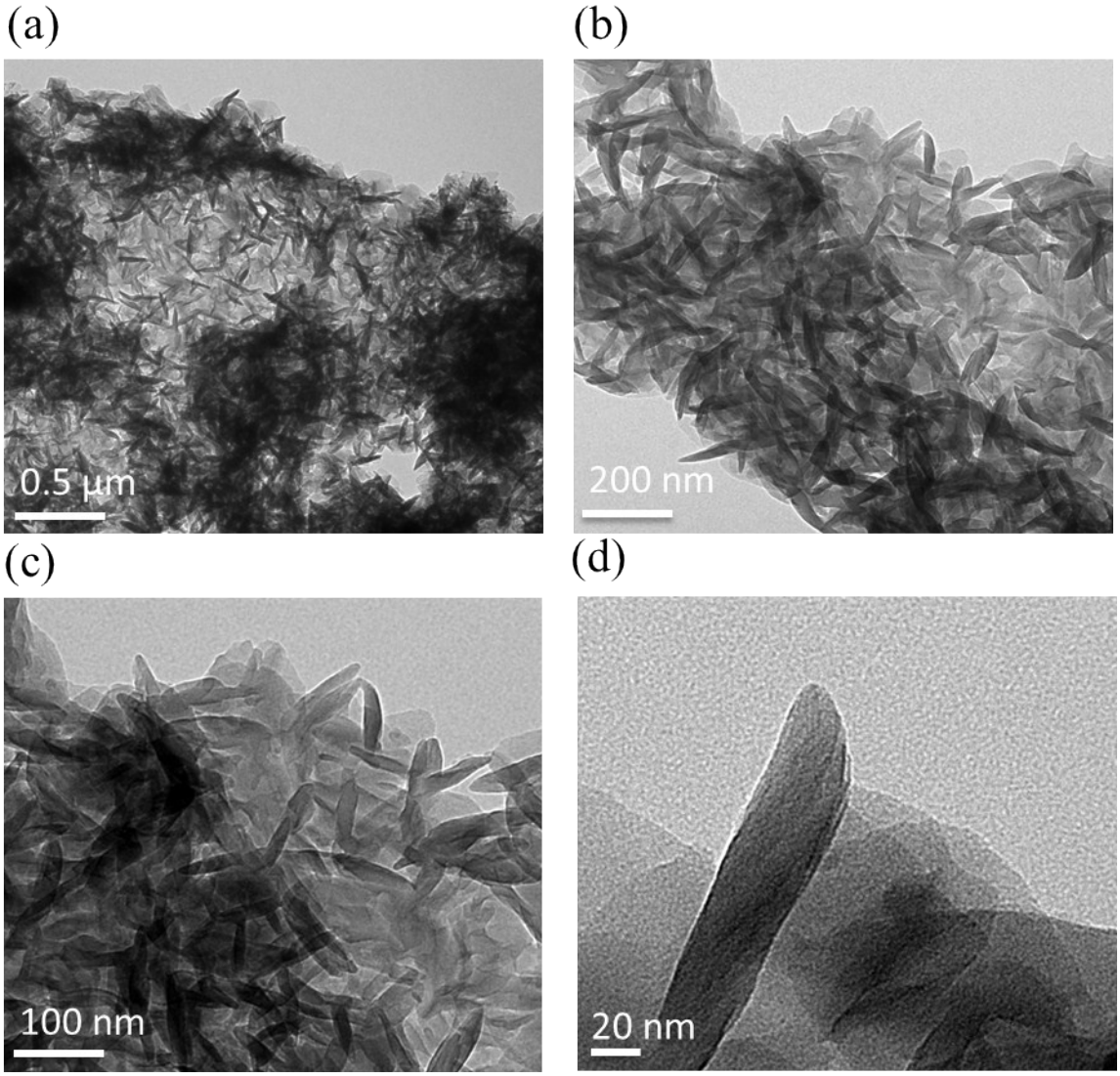

Fig. S10. TEM images of the TPPDA-TPTPE COF recorded at various magnifications: (a) 0.5 μm, (b) 200 nm, (c) 100 nm, and (d) 20 nm.

S9. Field Emission Scanning Electron Microscopy (FE-SEM)

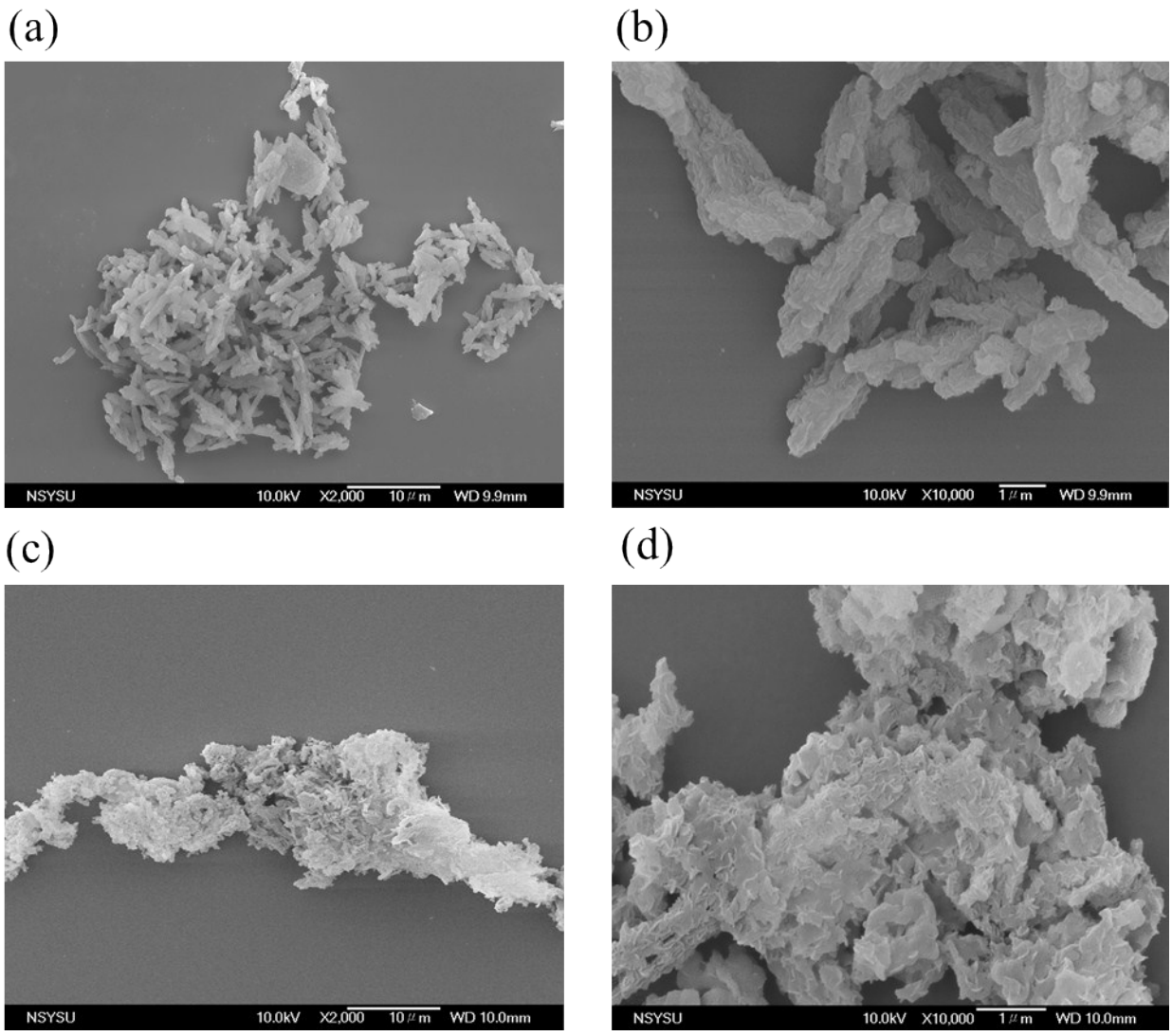

Fig. S11. FE-SEM images of the (a, b) TPPDA-TPPyr and (c, d) TPPDA-TPTPE COFs, recorded at various magnifications: (a, c) 10 and (b, d) 1 μm.

S10. Experimental and Simulation X-ray Diffraction Patterns for COFs Structures

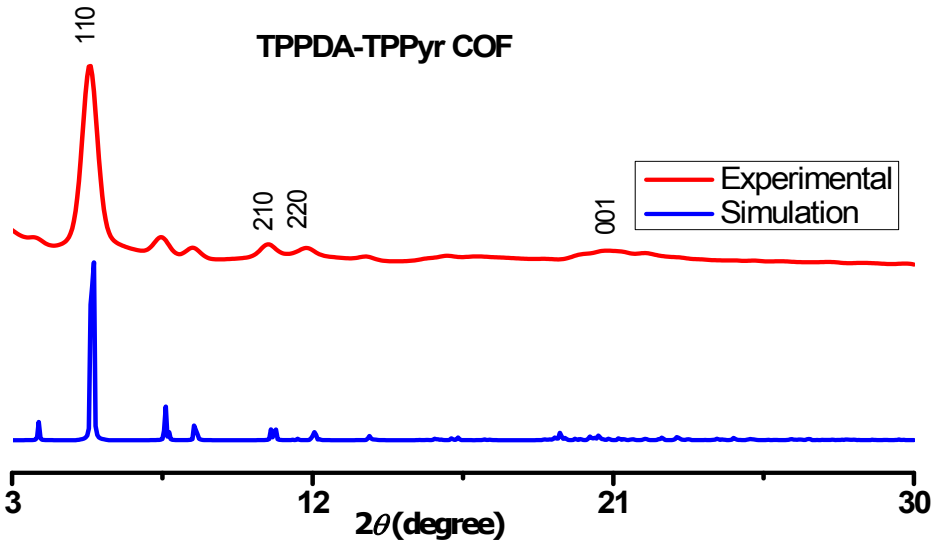

Fig. S12. PXRD pattern of the as-synthesized TPPDA-TPPyr COF (red), compared with the simulated PXRD pattern of the eclipsed AA-stacking model (blue).

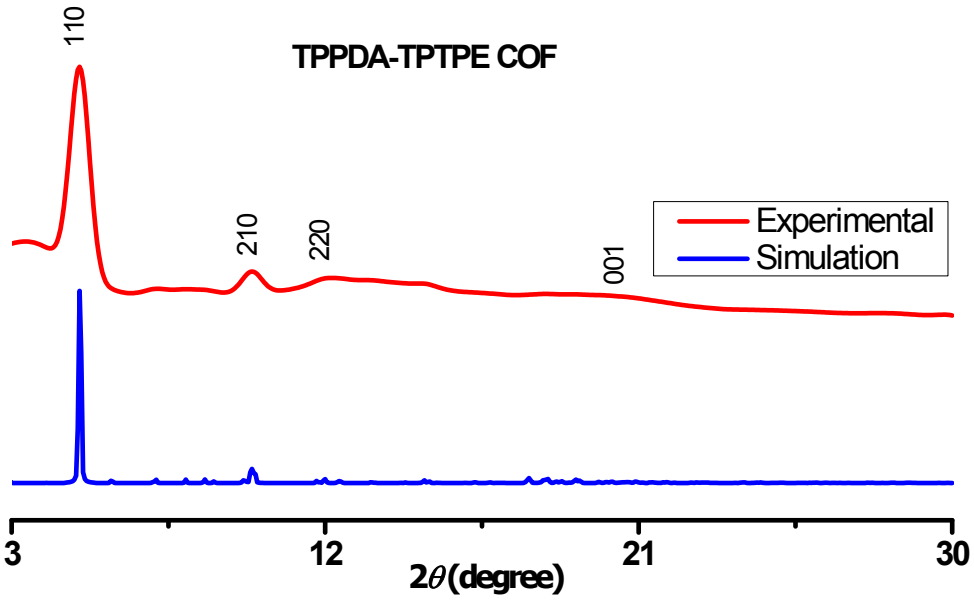

Fig. S13. PXRD pattern of the as-synthesized TPPDA-TPTPE COF (red), compared with the simulated PXRD pattern of the eclipsed AA-stacking model (blue).

S11. PXRD data and BET parameters

Table S2. PXRD data and BET parameters of the synthesized TPPDA-TPPyr and TPPDA-TPTPE COFs.

COFs	S_{BET} (m^2 g^{-1})	d_{100} (nm)	Pore size (nm)	Interlayer distance (Å)	Pore Volume (cm^3 g^{-1})
TPPDA-TPPyr COF	1020	1.66	1.25	4.2	0.66
TPPDA-TPTPE COF	1067	1.78	1.57	4.4	0.84

S12. Structural Modeling and Fractional atomic coordinates for COF Structures

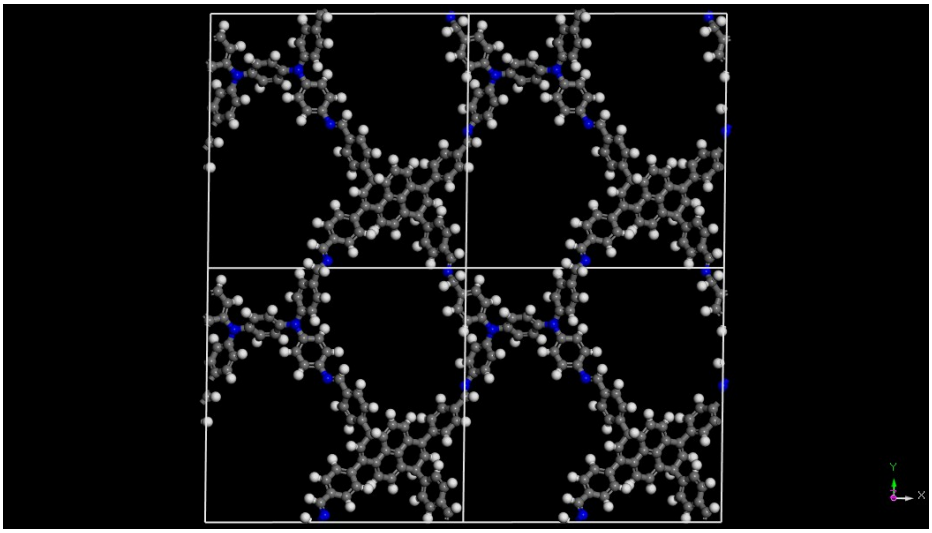

Fig. S14. 3D View along the *c*-axis of the simulated structure of the TPPDA-TPPyr COF.

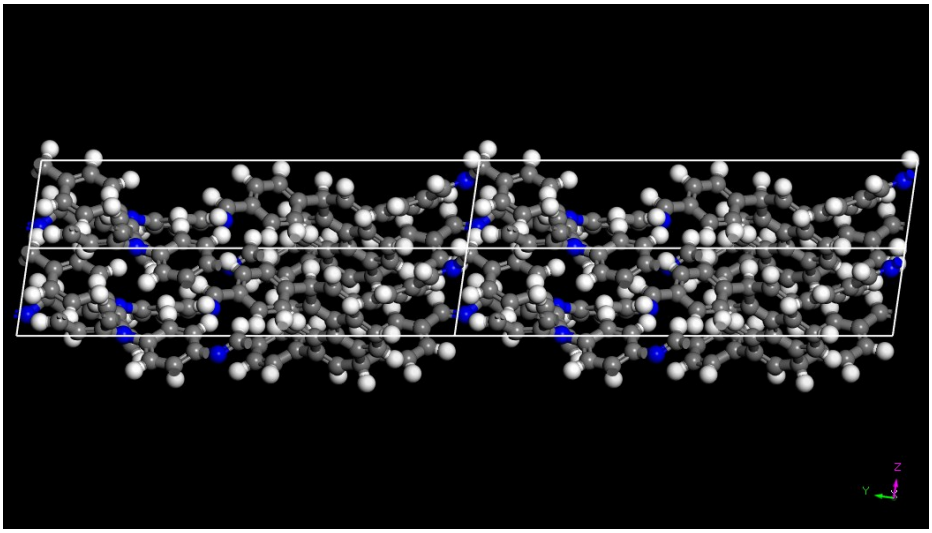

Fig. S15. 3D View along the *a*-axis of the simulated structure of the TPPDA-TPPyr COF.

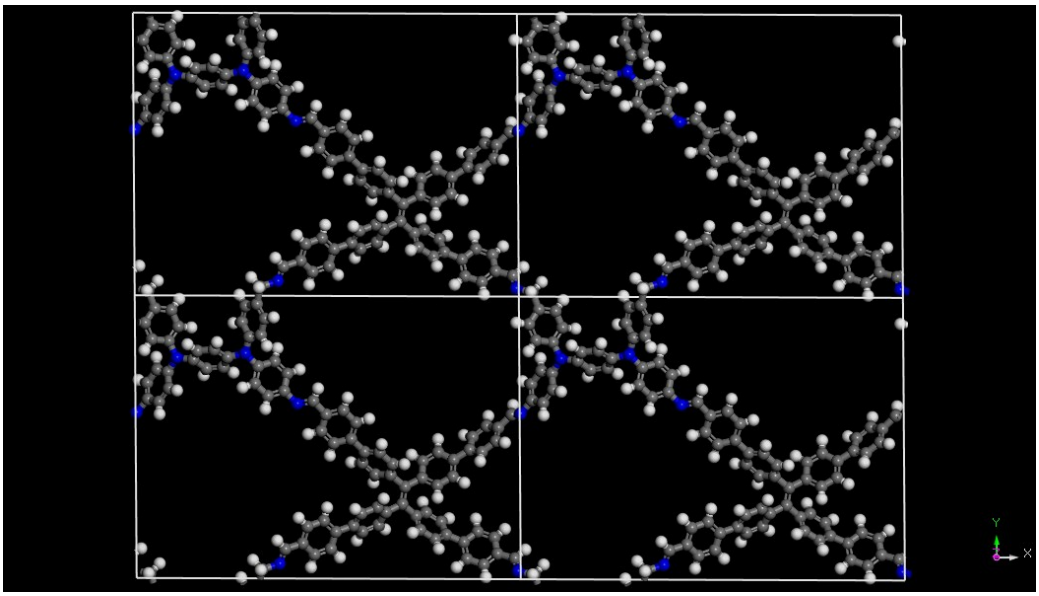

Fig. S16. 3D View along the *c*-axis of the simulated structure of the TPPDA-TPTPE COF.

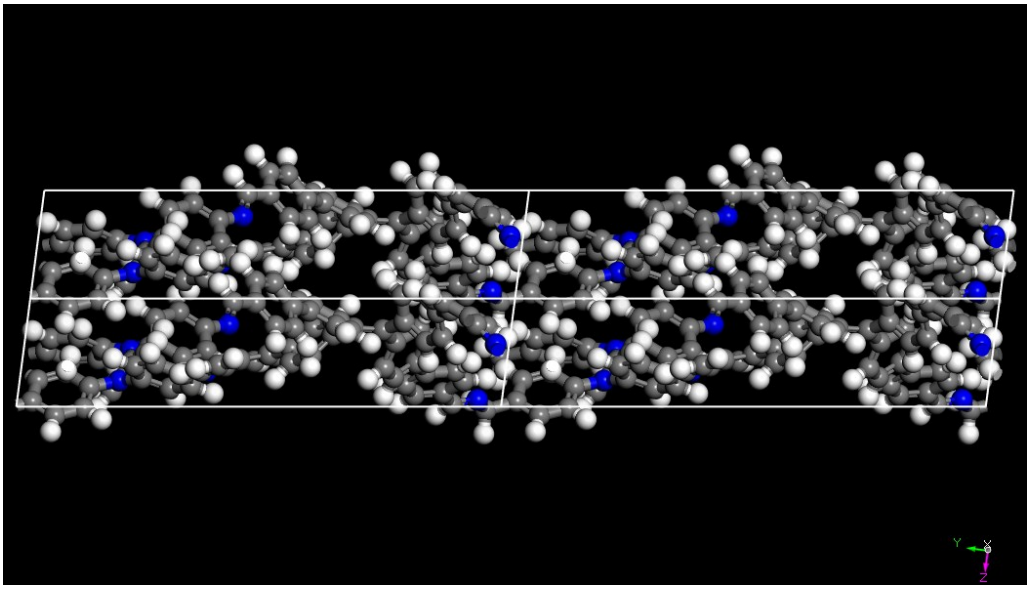

Fig. S17. 3D View along the *a*-axis of the simulated structure of the TPPDA-TPTPE COF.

Table S3. Fractional atomic coordinates for the unit cell of TPPDA-TPPyr COF with AA-stacking.

Sample name: TPPDA-TPPyr COF							
Space group: P1							
a = 23.72481 Å, b = 23.98233 Å, c = 4.51401 Å, α = 104.69º, β = 91.46º, γ = 90.11º							
R_{wp} = 18.47 %, R_p = 14.02 %							
Atom	***x/a***	***y/b***	***z/c***	**Atom**	***x/a***	***y/b***	***z/c***
N1	0.92811	-0.01674	0.23674	C21	0.63683	0.3453	0.5551
N2	0.46192	0.02701	0.76183	C22	0.59766	0.29393	0.54757
N3	0.33999	0.77687	0.32657	C23	0.60624	0.24252	0.38139
N4	0.1027	0.75695	0.00988	C24	0.60267	0.4006	0.53023
N5	0.46677	0.5643	0.31335	C25	0.56478	0.195	0.40611
N6	-0.00074	0.53522	-0.21487	C26	0.84969	0.16008	-0.18928
C7	0.65791	0.23402	0.19436	C27	0.87885	0.35642	-0.16675
C8	0.66926	0.18052	0.02411	C28	0.92748	0.35296	0.01169
C9	0.71837	0.17199	-0.14126	C29	0.96837	0.39702	0.04189
C10	0.75766	0.21683	-0.14742	C30	0.96165	0.44475	-0.10913
C11	0.74512	0.27232	0.0042	C31	0.91321	0.44779	-0.28991
C12	0.69562	0.2807	0.17977	C32	0.87187	0.40435	-0.31475
C13	0.7814	0.31955	-0.01837	C33	0.8406	0.10005	-0.26552
C14	0.76687	0.3748	0.12421	C34	0.87093	0.05953	-0.12386
C15	0.72066	0.38236	0.30821	C35	0.91242	0.07824	0.08893
C16	0.68449	0.33592	0.33819	C36	0.92364	0.13771	0.15427
C17	0.81228	0.20454	-0.31954	C37	0.89244	0.17799	0.01867
C18	0.84654	0.25879	-0.33994	C38	0.61429	0.45118	0.72392
C20	0.83457	0.31073	-0.18919	C39	0.58574	0.50346	0.69717

Continuous Table S3

Atom	***x/a***	***y/b***	***z/c***	**Atom**	***x/a***	***y/b***	***z/c***
C40	0.53133	0.45536	0.28927	C64	0.03233	0.58751	-0.17931
C41	0.56113	0.40322	0.31127	C65	0.07806	0.59788	0.0212
C42	0.50535	0.20621	0.39515	C66	0.10304	0.65295	0.07413
C43	0.46632	0.16597	0.47127	C67	0.0756	0.86184	0.0559
C44	0.48585	0.11352	0.55744	C68	0.03856	0.90773	0.16033
C45	0.54484	0.10051	0.55008	C69	-0.01386	0.89628	0.28183
C46	0.58382	0.1409	0.47591	C70	-0.03036	0.8385	0.28149
C47	0.94178	0.03781	0.26081	C71	0.00651	0.79286	0.17724
C48	1.00322	0.49263	-0.06285	C72	0.34472	0.66986	0.33151
C49	0.51454	0.56205	0.45875	C73	0.37605	0.61788	0.32398
C50	0.44522	0.07608	0.68222	C74	0.43554	0.61743	0.2963
C51	0.28042	0.77628	0.23374	C75	0.46339	0.66909	0.25917
C52	0.2386	0.80762	0.40526	C76	0.43187	0.72101	0.25978
C53	0.18039	0.80229	0.32932	C77	0.40396	0.83106	0.69798
C54	0.16287	0.76614	0.07824	C78	0.42644	0.88336	0.83782
C55	0.20477	0.73582	-0.09609	C79	0.40846	0.93669	0.75592
C56	0.26295	0.7414	-0.02052	C80	0.36942	0.93678	0.52531
C57	0.08306	0.69816	-0.07293	C81	0.34824	0.88436	0.38018
C58	0.06114	0.80388	0.07536	C82	0.42633	0.99325	0.92962
C59	0.36483	0.83079	0.4661	H83	0.63996	0.14467	0.0138
C60	0.37227	0.72245	0.30412	H84	0.72534	0.12986	-0.26737
C61	0.04008	0.68649	-0.28442	H85	0.79251	0.41237	0.10298
C62	0.01494	0.63164	-0.33704	H86	0.71315	0.42509	0.42791

Continuous Table S3

Atom	***x/a***	***y/b***	***z/c***	**Atom**	***x/a***	***y/b***	***z/c***
H87	0.79962	0.18617	-0.54345	H111	0.25093	0.83393	0.60556
H88	0.88667	0.25329	-0.45278	H112	0.14878	0.82437	0.47275
H89	0.65838	0.35049	0.76937	H113	0.19213	0.70777	-0.29052
H90	0.56178	0.29911	0.69326	H114	0.29471	0.71763	-0.15593
H91	0.93298	0.31716	0.13447	H115	0.02453	0.72095	-0.39768
H92	1.00472	0.39434	0.18723	H116	-0.01981	0.62386	-0.49363
H93	0.90671	0.48451	-0.40645	H117	0.09345	0.56484	0.14504
H94	0.83383	0.40882	-0.44312	H118	0.13595	0.66122	0.24021
H95	0.80949	0.08446	-0.43172	H119	0.11655	0.87155	-0.02965
H96	0.86167	0.01368	-0.17771	H120	0.05149	0.95226	0.15618
H97	0.95521	0.15329	0.31878	H121	-0.07091	0.82865	0.37132
H98	0.90142	0.22342	0.07959	H122	-0.00706	0.74892	0.18666
H99	0.64623	0.45042	0.89423	H123	0.29896	0.66908	0.36427
H100	0.59575	0.54185	0.84857	H124	0.35446	0.57805	0.3508
H101	0.4995	0.45665	0.11884	H125	0.50933	0.66898	0.22979
H102	0.55203	0.36499	0.15766	H126	0.45407	0.76032	0.23069
H103	0.48939	0.24728	0.33905	H127	0.41597	0.79079	0.7753
H104	0.42099	0.17676	0.47351	H128	0.45587	0.88234	1.01852
H105	0.5609	0.06033	0.61587	H129	0.35477	0.97759	0.46111
H106	0.62912	0.13078	0.4858	H130	0.31855	0.88543	0.20077
H107	0.97194	0.05576	0.42795	H131	0.45125	0.98526	1.12516
H108	1.03471	0.49271	0.10963	H132	0.38717	1.01808	1.00742
H109	0.53149	0.60126	0.58337	H133	-0.02236	0.96913	0.61086
H110	0.40207	0.09246	0.72771	H134	-0.08591	0.92766	0.5442

Table S4. Fractional atomic coordinates for the unit cell of TPPDA-TPTPE COF with AA-stacking.

Sample name: TPPDA-TPTPE COF							
Space group: P1							
a = 30.17763 Å, b = 22.29763 Å, c = 5.02702 Å, α = 82.62º, β = 86.04º, γ = 90.06º							
R_{wp} = 9.78%, R_p = 7.65%							
Atom	***x/a***	***y/b***	***z/c***	**Atom**	***x/a***	***y/b***	***z/c***
N1	0.37169	0.051	0.93628	C20	0.0566	0.73748	0.18672
N2	0.28559	0.79503	0.75984	C21	0.03027	0.69019	0.12617
N3	0.10767	0.77954	0.47859	C22	0.03189	0.63252	0.27619
N4	0.42018	0.61757	0.67401	C23	0.06072	0.62328	0.48391
N5	0.00169	0.58456	0.24294	C24	0.08695	0.67089	0.54532
N6	0.99173	0.02772	0.42358	C25	0.11239	0.89052	0.36015
C7	0.38697	0.10342	0.9746	C26	0.09457	0.94798	0.37198
C8	0.32664	1.03131	1.03204	C27	0.05141	0.9543	0.4869
C9	0.0347	1.01563	0.53607	C28	0.02558	0.90239	0.57742
C10	0.23988	0.78221	0.71571	C29	0.04321	0.84482	0.56122
C11	0.20538	0.8086	0.86069	C30	0.31092	0.6887	0.83027
C12	0.16154	0.80395	0.79459	C31	0.34426	0.6455	0.80774
C13	0.15109	0.77295	0.58148	C32	0.38687	0.66297	0.6972
C14	0.18481	0.74194	0.4512	C33	0.3955	0.72426	0.60258
C15	0.22909	0.74735	0.51465	C34	0.36235	0.76725	0.62529
C16	0.08441	0.72877	0.40016	C35	0.32725	0.86127	1.01544
C17	0.08725	0.83842	0.46031	C36	0.33751	0.91865	1.08011
C18	0.29741	0.85457	0.81914	C37	0.31732	0.97014	0.95278
C19	0.31964	0.75005	0.73791	C38	0.28753	0.96367	0.7559

Continuous Table S4

Atom	***x/a***	***y/b***	***z/c***	**Atom**	***x/a***	***y/b***	***z/c***
C39	0.27827	0.90649	0.68646	C64	0.77743	0.14043	0.35861
C40	0.46267	0.62793	0.6698	C65	0.80619	0.15626	0.12775
C41	0.97862	0.58165	0.03554	C66	0.79311	0.20207	-0.06987
C42	0.69959	0.32588	0.27559	C67	0.75411	0.23448	-0.0271
C43	0.69257	0.26445	0.29176	C68	0.51886	0.16525	0.68791
C44	0.64943	0.23549	0.40442	C69	0.56042	0.49385	0.52162
C45	0.7282	0.2226	0.21611	C70	0.8688	0.45721	0.07869
C46	0.74444	0.35643	0.20954	C71	0.85161	0.13027	0.11118
C47	0.66243	0.36706	0.34047	C72	0.57295	0.55232	0.56572
C48	0.66788	0.40609	0.53293	C73	0.54088	0.59511	0.61792
C49	0.63461	0.44641	0.59472	C74	0.49556	0.58065	0.62563
C50	0.59493	0.44893	0.4632	C75	0.48275	0.52224	0.58288
C51	0.58919	0.40948	0.27096	C76	0.51493	0.47915	0.53172
C52	0.62262	0.36889	0.21054	C77	0.9005	0.44947	0.27285
C53	0.78408	0.33076	0.30229	C78	0.93754	0.48802	0.25364
C54	0.8246	0.36209	0.25094	C79	0.94353	0.53526	0.04095
C55	0.82654	0.4213	0.11511	C80	0.91336	0.54113	-0.16017
C56	0.78693	0.44764	0.02791	C81	0.87652	0.50248	-0.14218
C57	0.74677	0.41579	0.07399	C82	0.48787	0.2041	0.79756
C58	0.62794	0.2521	0.63933	C83	0.44527	0.18341	0.89178
C59	0.58553	0.23006	0.72832	C84	0.43229	0.12379	0.87421
C60	0.56463	0.18739	0.59481	C85	0.46273	0.08495	0.76141
C61	0.58793	0.16647	0.37307	C86	0.50571	0.10534	0.67065
C62	0.63006	0.19001	0.28037	C87	0.85962	0.07091	0.22945
C63	0.73868	0.17298	0.40107	C88	0.90308	0.05089	0.26155

Continuous Table S4

Atom	***x/a***	***y/b***	***z/c***	**Atom**	***x/a***	***y/b***	***z/c***
C89	0.93935	0.08942	0.17184	H113	0.36993	0.81417	0.5528
C90	0.93158	0.14677	0.03425	H114	0.34212	0.82172	1.11882
C91	0.88819	0.16721	0.00584	H115	0.3605	0.92311	1.23289
C92	0.98483	0.07341	0.24385	H116	0.27151	1.00284	0.65571
H93	0.36593	0.13366	1.0787	H117	0.25581	0.90239	0.53077
H94	0.3227	1.0289	1.2546	H118	0.47499	0.67214	0.69832
H95	0.30258	1.06492	0.94599	H119	0.98243	0.61555	-0.13889
H96	0.0595	1.05148	0.4549	H120	0.69832	0.40501	0.63377
H97	0.03048	1.01645	0.75707	H121	0.6398	0.47527	0.74762
H98	0.21274	0.83466	1.0199	H122	0.55938	0.4111	0.16214
H99	0.13571	0.82682	0.90124	H123	0.6175	0.33951	0.06088
H100	0.17721	0.71741	0.28743	H124	0.78422	0.28661	0.41681
H101	0.25514	0.72721	0.39751	H125	0.8543	0.3399	0.32041
H102	0.05445	0.78169	0.07242	H126	0.78643	0.49395	-0.06742
H103	0.00775	0.69992	-0.03116	H127	0.717	0.43898	0.01234
H104	0.0616	0.57942	0.60383	H128	0.64406	0.28283	0.75195
H105	0.10771	0.66337	0.71341	H129	0.5695	0.24567	0.90568
H106	0.14635	0.88648	0.28087	H130	0.57297	0.13376	0.26407
H107	0.1151	0.98742	0.30107	H131	0.64694	0.17414	0.10582
H108	-0.00777	0.9068	0.66665	H132	0.7186	0.16229	0.58846
H109	0.02326	0.80521	0.63761	H133	0.78643	0.106	0.51714
H110	0.27843	0.6745	0.92123	H134	0.81386	0.21412	-0.25315
H111	0.33727	0.59836	0.87913	H135	0.74539	0.27149	-0.17436
H112	0.4275	0.73895	0.50633	H136	0.60764	0.56546	0.55445

Continuous Table S4

Atom	***x/a***	***y/b***	***z/c***	**Atom**	***x/a***	***y/b***	***z/c***
H137	0.55152	0.63995	0.64893	H145	0.42224	0.21422	0.97685
H138	0.4479	0.51025	0.58754	H146	0.45324	0.03871	0.74622
H139	0.50426	0.43427	0.50181	H147	0.52877	0.0739	0.59111
H140	0.89561	0.41585	0.44795	H148	0.8323	0.04071	0.3066
H141	0.96056	0.48258	0.41088	H149	0.90845	0.0062	0.366
H142	0.91765	0.57677	-0.32829	H150	0.9591	0.17715	-0.03735
H143	0.85376	0.50869	-0.3005	H151	0.88349	0.21336	-0.08346
H144	0.49632	0.25087	0.80824	H152	1.0119	0.10411	0.16584

Section 13. Electrochemical Analysis

Working Electrode Cleaning: Prior to use, the glassy carbon electrode (GCE) was polished several times with 0.05-μm alumina powder, washed with EtOH after each polishing step, cleaned via sonication (5 min) in a water bath, washed with EtOH, and then dried in air.

Electrochemical Characterization: The electrochemical experiments were performed in a three-electrode cell using an Autolab potentiostat (PGSTAT204) and 1 M KOH as the aqueous electrolyte. The GCE was used as the working electrode (diameter: 5.61 mm; 0.2475 cm^2). A Pt wire was used as the counter electrode; Hg/HgO (RE-61AP, BAS) was used as the reference electrode. All reported potentials refer to the Hg/HgO potential. The GCE was modified with COF slurries, as described elsewhere, but with some modifications.[S5–S7] The slurries were prepared by dispersing the COF (45 wt. %), carbon black (45 wt. %), and Nafion (10 wt. %) in EtOH (2 mL) and then sonicating for 1 h. A portion of this slurry (10 μL) was pipetted onto the tip of the electrode, which was then dried in air for 30 min prior to use. The electrochemical performance was studied through CV at various sweep rates (from 5 to 200 mV s^{-1}) and through the GCD method in the potential range from +0.18 to –0.92 V vs. Hg/HgO at various current densities (from 2 to 20 A g^{-1}) in 1 M KOH as the aqueous electrolyte solution.

The specific capacitance was calculated from the GCD data using the following equation:[S7,S8]

$$C_s = (I\Delta t)/(m\Delta V) \quad \text{(S1)}$$

where C_s (F g^{-1}) is specific capacitance of the supercapacitor, I (A) is the discharge current, ΔV (V) is the potential window, Δt (s) is the discharge time, and m (g) is the mass of the COF on the electrode. The energy density (E, W h kg^{-1}), and the power density (P, W kg^{-1}) were calculated using the following equations:[S4]

$$E = 1000C(\Delta V)^2/(2*3600) \quad \text{(S2)}$$

$$P = E/(t/3600) \quad \text{(S3)}$$

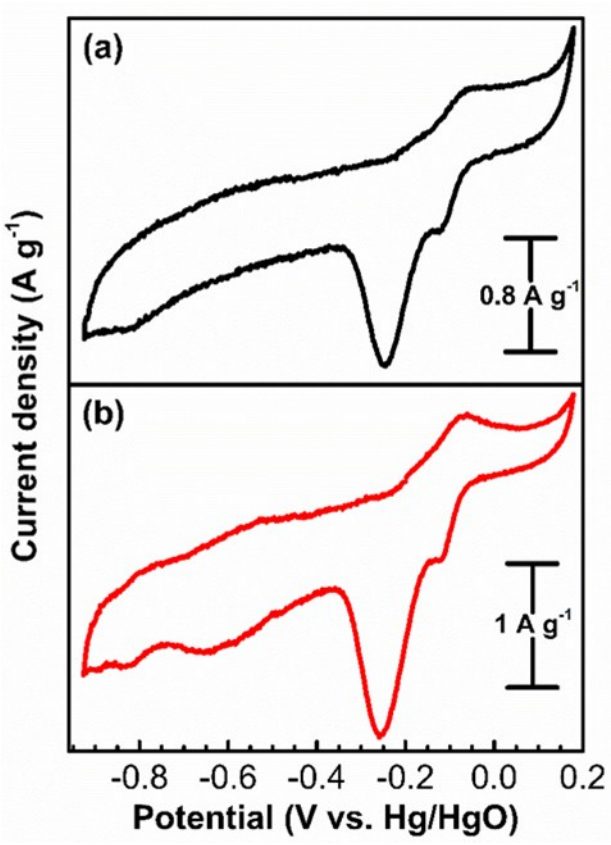

Fig. S18. Cyclic voltammograms of the (a) TPPDA-TPPyr and (b) TPPDA-TPTPE COFs recorded at scan rate of 5 mV s^{-1} in 1 M KOH.

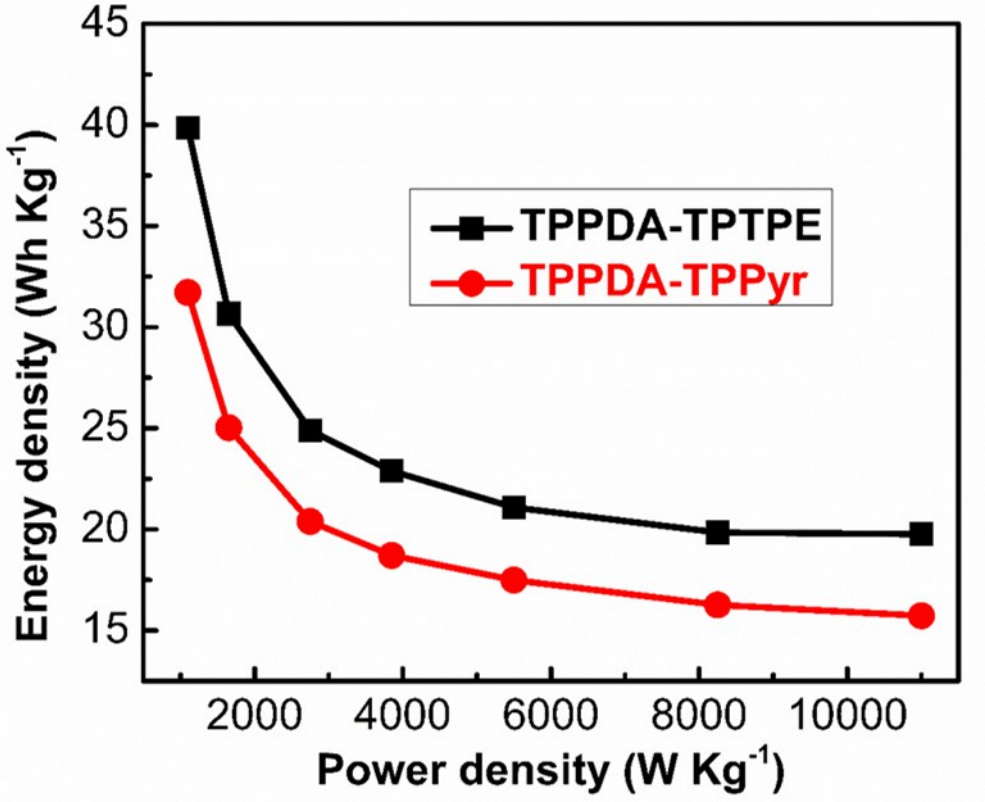

Fig. S19. Ragone plots of the energy density and power density of the TPPDA-TPPyr and TPPDA-TPTPE COF electrodes in 1 M KOH.

Table S5. Comparison between the specific surface area/specific capacitance of TPPDA–TPPyr and TPPDA–TPTPE COFs with those of previously reported COFs for supercapacitor application

COFs	S_{BET} ($m^2\ g^{-1}$)	Capacitance	Ref.
TPPDA–TPPyr	1020	188.7 F g^{-1} at 2 A g^{-1}	This work
TPPDA–TPTPE	1067	237.1 F g^{-1} at 2 A g^{-1}	This work
TPT–DAHQ COF	1855	181.1 F g^{-1} at 0.2 A g^{-1}	S5
Car–TPA COF	1334	13.6 F g^{-1} at 0.2 A g^{-1}	S6
Car–TPP COF	743	14.5 F g^{-1} at 0.2 A g^{-1}	S6
Car–TPT COF	721	17.4 F g^{-1} at 0.2 A g^{-1}	S6
DAAQ–TFP COF	1280	48 ± 10 F g^{-1} at 0.1 A g^{-1}	S7
TPA–COF–1	714	51.3 F g^{-1} at 0.2 A g^{-1}	S9
TPA–COF–2	478	14.4 F g^{-1} at 0.2 A g^{-1}	S9
TPA–COF–3	557	5.1 F g^{-1} at 0.2 A g^{-1}	S9
TPT–COF–4	1132	2.4 F g^{-1} at 0.2 A g^{-1}	S9
TPT–COF–5	1747	0.34 F g^{-1} at 0.2 A g^{-1}	S9
TPT–COF–6	1535	0.24 F g^{-1} at 0.2 A g^{-1}	S9
TaPay–Py COF	687	209 F g^{-1} at 0.5 A g^{-1}	S10
DAB–TFP COF	385	98 F g^{-1} at 0.5 A g^{-1}	S10

S14. References

S1. M. G. Rabbani, A. K. Sekizkardes, O. M. El-Kadri, B. R. Kaafarani and H. M. El-Kaderi, J. *Mater. Chem.,* 2012, **22(48)**, 25409.

S2. P. Rios, T. S. Carter, T. J. Mooibroek, M. P. Crump, M. Lisbjerg, M. Pittelkow, N. T. Supekar, G. J. Boons and A. P. Davis, *Angew. Chem. Int. Ed.* 2016, **55(10)**, 3387.

S3. X. Yunfeng, C. Dan, F. Shi, Z. Chong and J. Jia-Xing, *New J. Chem.,* 2016, **40**, 9415.

S4. L. Weijun, Z. Yixuan, Z. Jianyong, H. Jiajun, C. Zhenguo, M. W. Philip, C. Liuping and S. Cheng-Yong, *Chem. Commun.,* 2014, **50**, 11942.

S5. A. F. EL-Mahdy, Y. Hung, T. H. Mansoure, H.–H. Yu, T. Chen and S. Kuo, *Chem. Asian J.*, 2019, **14(9)**, 1429.

S6. A. F. M. EL-Mahdy, C. Young, J. Kim, J. You, Y. Yamauchi and S. W. Kuo, *ACS Appl. Mater. Interfaces*, 2019, **11(9)**, 9343.

S7. C. R. DeBlase, K. E. Silberstein, T.–T. Truong, H. D. Abruña and W. R. Dichtel, *J. Am. Chem. Soc.,* 2013, **135**, 16821.

S8. A. Alabadi, X. Yang, Z. Dong, Z. Li and B. Tan, *J. Mater. Chem. A,* 2014, **2**, 11697.

S9. A. F. M. El-Mahdy, C.-H. Kuo, A. A. Alshehri, J. Kim, C. Young, Y. Yamauchi and S.-W Kuo, *J. Mater. Chem. A* **2018**, 19532.

S10. A. M. Khattak, Z. A. Ghazi, B. Liang, N. A. Khan, A. Iqbal, L. Li and Z. Tang, *J. Mater. Chem. A*, 2016, **4**, 16312.